# $P_{cs}(4459)$ and other possible molecular states from $\Xi_c^{(*)}\bar{D}^{(*)}$ and $\Xi_c'\bar{D}^{(*)}$ interactions

Jun-Tao Zhu, Lin-Qing Song, and Jun He*

*Department of Physics and Institute of Theoretical Physics, Nanjing Normal University, Nanjing 210097, China*

(Received 1 February 2021; accepted 15 March 2021; published 12 April 2021)

Recently, the LHCb Collaboration reported a new structure $P_{cs}(4459)$ with a mass of 19 MeV below the $\Xi_c\bar{D}^*$ threshold. It may be a candidate of molecular state from the $\Xi_c\bar{D}^*$ interaction. In the current work, we perform a coupled-channel study of the $\Xi_c^*\bar{D}^*$, $\Xi_c'\bar{D}^*$, $\Xi_c^*\bar{D}$, $\Xi_c\bar{D}^*$, $\Xi_c'\bar{D}$, and $\Xi_c\bar{D}$ interactions in the quasipotential Bethe-Salpeter equation approach. With the help of the heavy quark chiral effective Lagrangian, the potential is constructed by light meson exchanges. Two $\Xi_c\bar{D}^*$ molecular states are produced with spin parities $J^P = 1/2^-$ and $3/2^-$. The lower state with $3/2^-$ can be related to the observed $P_{cs}(4450)$ while two-peak structure cannot be excluded. Within the same model, other strange hidden-charm pentaquarks are also predicted. Two states with spin parities $1/2^-$ and a state with $3/2^-$ are predicted near the $\Xi_c'\bar{D}$, $\Xi_c\bar{D}$, and $\Xi_c^*\bar{D}$ thresholds, respectively. As two states near $\Xi_c\bar{D}^*$ threshold, two states are produced with $1/2^-$ and $3/2^-$ near the $\Xi_c'\bar{D}^*$ threshold. The couplings of the molecular states to the considered channels are also discussed. The experimental research of those states are helpful to understand the origin and internal structure of the $P_{cs}$ and $P_c$ states.

DOI: 10.1103/PhysRevD.103.074007

## I. INTRODUCTION

Recently, the LHCb Collaboration released their results about the $\Xi_b \to J/\psi K^-\Lambda$ decay, which indicates a new resonance structure named $P_{cs}(4459)$, which carries a mass of $4458.8 \pm 2.9^{+4.7}_{-1.1}$ MeV and a width of $17.3 \pm 6.5^{+8.0}_{-5.7}$ MeV [1]. Such structure is just 19 MeV below the $\Xi_c\bar{D}^*$ threshold and the width is relatively narrow. It follows a series of observations about the hidden-charm pentaquarks. In 2015, the LHCb Collaboration firstly reported two structures $P_c(4380)$ and $P_c(4450)$ in the $\Lambda_b \to J/\psi K^- p$ [2], which are close to the $\Sigma_c^*\bar{D}$ and $\Sigma_c\bar{D}^*$ thresholds, respectively. Such observation confirmed previous predictions about the hidden-charm pentaquarks [3–6]. Due to the closeness to the thresholds, these structures were soon interpreted as molecular states in the literature [7–12]. Other pictures, such as compact pentaquark [13–15] and anomalous triangle singularity [16], were also proposed to explain the observation. In 2019, the LHCb Collaboration updated their results. The upper $P_c(4450)$ was found to be a two-peak structure named as $P_c(4457)$ and $P_c(4440)$, and a new structure, $P_c(4312)$, was observed near $\Sigma_c\bar{D}$ threshold [17]. The new result strongly supports the molecular state picture. If we include the $P_c(4380)$ state, which was not confirmed but also not excluded by new observation, the four states provide a wonderful spectrum of S-wave states from the $\Sigma_c\bar{D} - \Sigma_c^*\bar{D} - \Sigma_c\bar{D}^*$ interaction. Based on such observation, in Refs. [18–20] all possible S-wave molecular states from not only above channels but also the $\Sigma_c^*D^*$ channel were included in the study. With these states, the experimental data were well reproduced.

The observation of the hidden-charm pentaquarks inspires a large amount of theoretical studies about their internal structure [21–31]. The partners of the hidden-charm pentaquarks were also widely discussed in the literature [32–40]. Replacing one of the light quark by strange quark, one can naturally obtain a strange hidden-charm pentaquark, which have been studied in the pioneer work [3] and some studies after the observation of $P_c$ states [41–50]. The observation of these partners is very helpful to understand the internal structure of the pentaquarks.

The recent observation of $P_{cs}(4459)$ favors the molecular state interpretations of the hidden-charm pentaquarks [51–54]. It can be taken as the strange partner of the $P_c(4450)$. According to its mass, it can be assigned as the candidate of a $\Xi_c\bar{D}^*$ state with spin parity $J^P = 1/2^-$ or $3/2^-$. Due to lack of the partial-wave treatment, the current

*Corresponding author.
junhe@njnu.edu.cn

experimental analysis did not provide the information about its spin parity. From the experience of study about the $P_c(4450)$, one can expect that there may be two structures in the $P_{cs}(4459)$. The two-pole structure of a resonance was first proposed in the study of the $\Lambda(1405)$ [55,56], and also suggested in the studies of $K_1(1270)$ and $D_0^*(2400)$ [57–59]. In Ref. [49], the author predicted two $\Xi_c\bar{D}^*$ states with $J^P = 1/2^-$ and $3/2^-$ which carry masses of $4456.9^{+3.2}_{-3.3}$ and $4463^{+2.8}_{-3.0}$ MeV, respectively. Different mass order of two $\Xi_c\bar{D}^*$ states was also suggested in the literature. In Ref. [52], the calculation yields masses of 4469 and 4453–4463 MeV for states with $1/2$ and $3/2$, respectively.

In our previous work, the hidden-charm pentaquarks were well explained as molecular states in the quasipotential Bethe-Salpeter equation (qBSE) approach [28,29], which was extended to predict the hidden-bottom pentaquarks [40]. Such studies provide a good theoretical frame to study the strange hidden-charm pentaquark. Due to the heavy quark symmetry, the model has been constrained by experimentally observed hidden-charm pentaquarks. Hence, it is interesting to perform a calculation about the molecular states from the $\Xi_c^{(*,\prime)}\bar{D}^{(*)}$ interaction in the same frame. The strange hidden-charm pentaquarks are also possibly produced from the interactions of charmed baryon and strange anticharm meson. Compared with the couplings between channels in the $\Xi_c^{(*,\prime)}\bar{D}^{(*)}$ interactions where the pion exchange is possible, the couplings between two types of interactions through kaon exchange should be weaker. Hence, in the current work, we consider six channels in $\Xi_c^{(*,\prime)}\bar{D}^{(*)}$ interaction, which are related to the $P_{cs}(4459)$.

With the help of the heavy quark chiral effective Lagrangians, which was also adopted to reproduce the hidden-charm pentaquarks, the one-boson-exchange model will be adopted in the current work to construct the interaction kernel to calculate the scattering amplitude by solving the qBSE. The molecular states can be studied by searching for the poles of the complex energy plane. The coupled-channel effects will be also included explicitly to produce the widths of the molecular states. The molecular state interpretation of the $P_{cs}(4459)$ will be discussed based on the results. More molecular states will be also predicted, which can be searched in the future experiment.

This article is organized as follows. After introduction, Sec. II shows the details of dynamics of the $\Xi_c^*\bar{D}^*$, $\Xi_c'\bar{D}^*$, $\Xi_c^*\bar{D}$, $\Xi_c\bar{D}^*$, $\Xi_c'\bar{D}$, and $\Xi_c\bar{D}$ interactions, including the relevant effective Lagrangians, reduction of potential kernel and a brief introduction of the qBSE. In Sec. III, the results with single-channel calculation are given first. Then, coupled-channel results are presented, and the importance of the channels considered are discussed. Finally, summary and discussion are given in Section III B.

## II. THEORETICAL FRAME

In the current work, we follows the same theoretical frame in the study of the LHCb hidden-charm pentaquarks [28,29], to study the strange hidden-charm pentaquark. The one-boson-exchange potential of the interactions of strange charmed baryon $\Xi_c^{(*,\prime)}$ and anticharm meson $\bar{D}^{(*)}$ is constructed as dynamical kernel. The pseudoscalar $\mathbb{P}$, vector $\mathbb{V}$ and scalar $\sigma$ exchanges will be considered, and the effective Lagrangian depicting the couplings of light mesons and anticharmed mesons $\bar{D}^{(*)}$ or strange charmed baryons $\Xi_c^{(*,\prime)}$ are required and will be presented in the below.

### A. Relevant Lagrangians

First, we consider the couplings of light mesons and heavy-light anticharmed mesons $\mathcal{P} = (\bar{D}^0, D^-, D_s^-)$. Considering heavy quark limit and chiral symmetry, the Lagrangians have been constructed in the literature as [60–63],

$$\begin{aligned}
\mathcal{L}_{HH\mathbb{P}} &= ig\langle \bar{H}_a^{\bar{Q}}\gamma_\mu \mathcal{A}^\mu_{ba}\gamma_5 H_b^{\bar{Q}}\rangle,\\
\mathcal{L}_{HH\mathbb{V}} &= -i\beta\langle \bar{H}_a^{\bar{Q}} v_\mu(\mathcal{V}^\mu_{ab} - \rho^\mu_{ab})H_b^{\bar{Q}}\rangle\\
&\quad + i\lambda\langle \bar{H}_b^{\bar{Q}}\sigma_{\mu\nu}F^{\mu\nu}(\rho)\bar{H}_a^{\bar{Q}}\rangle,\\
\mathcal{L}_{HH\sigma} &= g_s\langle \bar{H}_a^{\bar{Q}}\sigma\bar{H}_a^{\bar{Q}}\rangle,
\end{aligned} \tag{1}$$

where $\mathcal{A}^\mu = \frac{1}{2}(\xi^\dagger\partial_\mu\xi - \xi\partial_\mu\xi^\dagger) = \frac{i}{f_\pi}\partial_\mu\mathbb{P} + \cdots$ is the axial current with $\xi = \exp(i\mathbb{P}/f_\pi)$ and $f_\pi = 132$ MeV. $\mathcal{V}_\mu = \frac{i}{2}[\xi^\dagger\partial_\mu\xi + \xi\partial^\mu\xi^\dagger] = \frac{i}{2f_\pi^2}[\mathbb{P}, \partial_\mu\mathbb{P}] + \cdots$, which is irreverent to the interactions in the current work. $\rho^\mu_{ba} = ig_{\mathbb{V}}\mathbb{V}^\mu_{ba}/\sqrt{2}$, and $F^{\mu\nu}(\rho) = \partial_\mu\rho_\nu - \partial_\nu\rho_\mu + [\rho_\mu, \rho_\nu]$. The $\mathbb{P}$ and $\mathbb{V}$ are the pseudoscalar and vector matrices as

$$\mathbb{P} = \begin{pmatrix} \frac{1}{\sqrt{2}}\pi^0 + \frac{\eta}{\sqrt{6}} & \pi^+ & K^+ \\ \pi^- & -\frac{1}{\sqrt{2}}\pi^0 + \frac{\eta}{\sqrt{6}} & K^0 \\ K^- & \bar{K}^0 & -\frac{2\eta}{\sqrt{6}} \end{pmatrix},$$

$$\mathbb{V} = \begin{pmatrix} \frac{\rho^0}{\sqrt{2}} + \frac{\omega}{\sqrt{2}} & \rho^+ & K^{*+} \\ \rho^- & -\frac{\rho^0}{\sqrt{2}} + \frac{\omega}{\sqrt{2}} & K^{*0} \\ K^{*-} & \bar{K}^{*0} & \phi \end{pmatrix}. \tag{2}$$

The doublet is defined as $H_a^{\bar{Q}} = [\mathcal{P}_a^{*\mu}\gamma_\mu - \mathcal{P}_a^{\bar{Q}}\gamma_5]\frac{1-\not{v}}{2}$ and $\bar{H} = \gamma_0 H^\dagger \gamma_0$. The $\mathcal{P}$ and $\mathcal{P}^*$ satisfy the normalization relations $\langle 0|\mathcal{P}|\bar{Q}q(0^-)\rangle = \sqrt{M_{\mathcal{P}}}$ and $\langle 0|\mathcal{P}^*_\mu|\bar{Q}q(1^-)\rangle = \epsilon_\mu\sqrt{M_{\mathcal{P}^*}}$. The $\langle\cdots\rangle$ denotes the trace for the Dirac gamma matrices.

The Lagrangians can be further expanded as follows for explicitly application,

$$
\begin{aligned}
\mathcal{L}_{\mathcal{P}^*\mathcal{P}\mathbb{P}} &= i\frac{2g}{f_\pi}(-\mathcal{P}^{*\dagger}_{a\lambda}\mathcal{P}_b + \mathcal{P}^\dagger_a\mathcal{P}^*_{b\lambda})\partial^\lambda\mathbb{P}_{ab},\\
\mathcal{L}_{\mathcal{P}^*\mathcal{P}^*\mathbb{P}} &= -\frac{g}{f_\pi\sqrt{m_\mathcal{P} m_{\mathcal{P}^*}}}\epsilon_{\alpha\mu\nu\lambda}\mathcal{P}^{*\mu\dagger}_a\overleftrightarrow{\partial}^\alpha\mathcal{P}^{*\lambda}_b\partial^\nu\mathbb{P}_{ba},\\
\mathcal{L}_{\mathcal{P}^*\mathcal{P}\mathbb{V}} &= \frac{\sqrt{2}\lambda g_V}{\sqrt{m_\mathcal{P} m_{\mathcal{P}^*}}}\epsilon_{\lambda\alpha\beta\mu}(-\mathcal{P}^{*\mu\dagger}_a\overleftrightarrow{\partial}^\lambda\mathcal{P}_b + \mathcal{P}^\dagger_a\overleftrightarrow{\partial}^\lambda\mathcal{P}^{*\mu}_b)\\
&\quad\times(\partial^\alpha\mathbb{V}^\beta)_{ab},\\
\mathcal{L}_{\mathcal{P}\mathcal{P}\mathbb{V}} &= -i\frac{\beta g_V}{\sqrt{2}\sqrt{m_\mathcal{P} m_{\mathcal{P}^*}}}\mathcal{P}^\dagger_a\overleftrightarrow{\partial}_\mu\mathcal{P}_b\mathbb{V}^\mu_{ab},\\
\mathcal{L}_{\mathcal{P}^*\mathcal{P}^*\mathbb{V}} &= -i\frac{\beta g_V}{\sqrt{2}\sqrt{m_\mathcal{P} m_{\mathcal{P}^*}}}\mathcal{P}^{*\dagger}_a\overleftrightarrow{\partial}_\mu\mathcal{P}^*_b\mathbb{V}^\mu_{ab}\\
&\quad - i2\sqrt{2}\lambda g_V\mathcal{P}^{*\mu\dagger}_a\mathcal{P}^{*\nu}_b(\partial_\mu\mathbb{V}_\nu - \partial_\nu\mathbb{V}_\mu)_{ab},\\
\mathcal{L}_{\mathcal{P}\mathcal{P}\sigma} &= -2g_s\mathcal{P}^\dagger_a\mathcal{P}_a\sigma,\\
\mathcal{L}_{\mathcal{P}^*\mathcal{P}^*\sigma} &= 2g_s\mathcal{P}^{*\dagger}_a\mathcal{P}^*_a\sigma,
\end{aligned}
\tag{3}
$$

where the $v$ is replaced by $i\overleftrightarrow{\partial}/2\sqrt{m_i m_f}$ with the $m_{i,f}$ is for the initial or final $\bar{D}^{(*)}$ meson.

The Lagrangians for the couplings between charmed baryon and light mesons can also be constructed under the heavy quark limit and chiral symmetry as [64],

$$
\begin{aligned}
\mathcal{L}_S &= -\frac{3}{2}g_1(v_\kappa)\epsilon^{\mu\nu\lambda\kappa}\mathrm{tr}[\bar{S}_\mu\mathcal{A}_\nu S_\lambda] + i\beta_S\mathrm{tr}[\bar{S}_\mu v_\alpha(\mathcal{V}^\alpha - \rho^\alpha)S^\mu]\\
&\quad + \lambda_S\mathrm{tr}[\bar{S}_\mu F^{\mu\nu}S_\nu] + \ell_S\mathrm{tr}[\bar{S}_\mu\sigma S^\mu],\\
\mathcal{L}_{B_{\bar{3}}} &= i\beta_B\mathrm{tr}[\bar{B}_{\bar{3}}v_\mu(\mathcal{V}^\mu - \rho^\mu)B_{\bar{3}}] + \ell_B\mathrm{tr}[\bar{B}_{\bar{3}}\sigma B_{\bar{3}}],\\
\mathcal{L}_{\mathrm{int}} &= ig_4\mathrm{tr}[\bar{S}^\mu\mathcal{A}_\mu B_{\bar{3}}] + i\lambda_I\epsilon^{\mu\nu\lambda\kappa}v_\mu\mathrm{tr}[\bar{S}_\nu F_{\lambda\kappa}B_{\bar{3}}] + \mathrm{H.c.},
\end{aligned}
\tag{4}
$$

where $S^\mu_{ab}$ is composed of Dirac spinor operators,

$$
\begin{aligned}
S^{ab}_\mu &= -\sqrt{\frac{1}{3}}(\gamma_\mu + v_\mu)\gamma^5 B^{ab} + B^{*ab}_\mu \equiv B^{ab}_{0\mu} + B^{ab}_{1\mu},\\
\bar{S}^{ab}_\mu &= \sqrt{\frac{1}{3}}\bar{B}^{ab}\gamma^5(\gamma_\mu + v_\mu) + \bar{B}^{*ab}_\mu \equiv \bar{B}^{ab}_{0\mu} + \bar{B}^{ab}_{1\mu},
\end{aligned}
\tag{5}
$$

and the bottomed baryon matrices are defined as

$$
B_{\bar{3}} = \begin{pmatrix} 0 & \Lambda_c^+ & \Xi_c^+ \\ -\Lambda_c^+ & 0 & \Xi_c^0 \\ -\Xi_c^+ & -\Xi_c^0 & 0 \end{pmatrix},
$$

$$
B = \begin{pmatrix} \Sigma_c^{++} & \frac{1}{\sqrt{2}}\Sigma_c^+ & \frac{1}{\sqrt{2}}\Xi_c^{\prime+} \\ \frac{1}{\sqrt{2}}\Sigma_c^+ & \Sigma_c^0 & \frac{1}{\sqrt{2}}\Xi_c^{\prime0} \\ \frac{1}{\sqrt{2}}\Xi_c^{\prime+} & \frac{1}{\sqrt{2}}\Xi_c^{\prime0} & \Omega_c^0 \end{pmatrix}.
$$

$$
B^* = \begin{pmatrix} \Sigma_c^{*++} & \frac{1}{\sqrt{2}}\Sigma_c^{*+} & \frac{1}{\sqrt{2}}\Xi_c^{*+} \\ \frac{1}{\sqrt{2}}\Sigma_c^{*+} & \Sigma_c^{*0} & \frac{1}{\sqrt{2}}\Xi_c^{*0} \\ \frac{1}{\sqrt{2}}\Xi_c^{*+} & \frac{1}{\sqrt{2}}\Xi_c^{*0} & \Omega_c^{*0} \end{pmatrix}.
\tag{6}
$$

TABLE I. The coupling constants adopted in the calculation, which are cited from the literature [21,64,66,67]. The $\lambda$ and $\lambda_{S,I}$ are in the units of $\mathrm{GeV}^{-1}$. Others are in the units of 1.

| $\beta$ | $g$ | $g_V$ | $\lambda$ | $g_s$ |
|---|---|---|---|---|
| 0.9 | 0.59 | 5.9 | 0.56 | 0.76 |

| $\beta_S$ | $\ell_S$ | $g_1$ | $\lambda_S$ | $\beta_B$ | $\ell_B$ | $g_4$ | $\lambda_I$ |
|---|---|---|---|---|---|---|---|
| −1.74 | 6.2 | −0.94 | −3.31 | $-\beta_S/2$ | $-\ell_S/2$ | $3g_1/(2\sqrt{2})$ | $-\lambda_S/\sqrt{8}$ |

The explicit forms of the Lagrangians can be written as,

$$
\begin{aligned}
\mathcal{L}_{BB\mathbb{P}} &= -i\frac{3g_1}{4f_\pi\sqrt{m_{\bar{B}}m_B}}\epsilon^{\mu\nu\lambda\kappa}\partial^\nu\mathbb{P}\sum_{i=0,1}\bar{B}_{i\mu}\overleftrightarrow{\partial}_\kappa B_{j\lambda},\\
\mathcal{L}_{BB\mathbb{V}} &= -\frac{\beta_S g_V}{2\sqrt{2m_{\bar{B}}m_B}}\mathbb{V}^\nu\sum_{i=0,1}\bar{B}^\mu_i\overleftrightarrow{\partial}_\nu B_{j\mu}\\
&\quad -\frac{\lambda_S g_V}{\sqrt{2}}(\partial_\mu\mathbb{V}_\nu - \partial_\nu\mathbb{V}_\mu)\sum_{i=0,1}\bar{B}^\mu_i B^\nu_j,\\
\mathcal{L}_{BB\sigma} &= \ell_S\sigma\sum_{i=0,1}\bar{B}^\mu_i B_{j\mu},\\
\mathcal{L}_{B_{\bar{3}}B_{\bar{3}}\mathbb{V}} &= -\frac{g_V\beta_B}{2\sqrt{2m_{\bar{B}_{\bar{3}}}m_{B_{\bar{3}}}}}\mathbb{V}^\mu\bar{B}_{\bar{3}}\overleftrightarrow{\partial}_\mu B_{\bar{3}},\\
\mathcal{L}_{B_{\bar{3}}B_{\bar{3}}\sigma} &= i\ell_B\sigma\bar{B}_{\bar{3}}B_{\bar{3}},\\
\mathcal{L}_{BB_{\bar{3}}\mathbb{P}} &= -i\frac{g_4}{f_\pi}\sum_i\bar{B}^\mu_i\partial_\mu\mathbb{P}B_{\bar{3}} + \mathrm{H.c.},\\
\mathcal{L}_{BB_{\bar{3}}\mathbb{V}} &= \frac{g_\mathbb{V}\lambda_I}{\sqrt{2m_{\bar{B}}m_{B_{\bar{3}}}}}\epsilon^{\mu\nu\lambda\kappa}\partial_\lambda\mathbb{V}_\kappa\sum_i\bar{B}_{i\nu}\overleftrightarrow{\partial}_\mu B_{\bar{3}} + \mathrm{H.c.}
\end{aligned}
\tag{7}
$$

The masses of particles involved in the calculation are chosen as suggested central values in the Review of Particle Physics (PDG) [65]. The mass of broad $\sigma$ meson is chosen as 500 MeV. The coupling constants involved are listed in Table I.

With the vertices obtained from above Lagrangians, the potential of couple-channel interaction can be constructed easily with the help of the standard Feynman rules. Because six channels are involved in the current work, it is tedious and fallible to give explicit 36 potential elements and input them into code. Instead, in this work, following the method in Ref. [29], we input vertices $\Gamma$ and propagators $P$ into the code directly. The potential can be written as

$$
\mathcal{V}_{\mathbb{P},\sigma} = f_I\Gamma_1\Gamma_2 P_{\mathbb{P},\sigma}f(q^2), \qquad \mathcal{V}_\mathbb{V} = f_I\Gamma_{1\mu}\Gamma_{2\nu}P^{\mu\nu}_\mathbb{V}f(q^2),
\tag{8}
$$

The propagators are defined as usual as

TABLE II. The flavor factors $f_I$ for certain meson exchanges of certain interaction. The values in bracket are for the case of $I = 1$ if the values are different from these of $I = 0$.

| | $\pi$ | $\eta$ | $\rho$ | $\omega$ | $\sigma$ |
|---|---|---|---|---|---|
| $\bar{D}^{(*)}\Xi_c^{(\prime,*)} \to \bar{D}^{(*)}\Xi_c^{(\prime,*)}$ | $-\frac{3}{4}\left[\frac{1}{4}\right]$ | $\frac{1}{6}$ | $-\frac{3}{4}\left[\frac{1}{4}\right]$ | $\frac{1}{2}$ | 1 |
| $\bar{D}^{(*)}\Xi_c \to \bar{D}^{(*)}\Xi_c$ | 0 | 0 | $-\frac{3}{2}\left[\frac{1}{2}\right]$ | $\frac{1}{2}$ | 2 |
| $\bar{D}^{(*)}\Xi_c \to \bar{D}^{(*)}\Xi_c^{(\prime,*)}$ | $-\frac{3}{2\sqrt{2}}\left[\frac{1}{2\sqrt{2}}\right]$ | $\frac{-1}{2\sqrt{2}}$ | $-\frac{3}{2\sqrt{2}}\left[\frac{1}{2\sqrt{2}}\right]$ | $\frac{1}{2\sqrt{2}}$ | 0 |

$$P_{\mathbb{P},\sigma} = \frac{i}{q^2 - m^2_{\mathbb{P},\sigma}}, \qquad P^{\mu\nu}_{\mathbb{V}} = i\frac{-g^{\mu\nu} + q^\mu q^\nu/m^2_{\mathbb{V}}}{q^2 - m^2_{\mathbb{V}}}, \quad (9)$$

where the form factor $f(q^2)$ is adopted to compensate the off-shell effect of exchanged meson as $f(q^2) = e^{-(m_e^2-q^2)^2/\Lambda_e^2}$ with $m_e$ being the $m_{\mathbb{P},\mathbb{V},\sigma}$ and $q$ being the momentum of the exchanged meson. The $f_I$ is the flavor factor for certain meson exchange of certain interaction, and the explicit values are listed in Table II.

With the potential kernel obtained, we adopt the qBSE to solve the scattering amplitude [32,33,68–70]. After partial-wave decomposition and spectator quasipotential approximation, the 4-dimensional Bethe-Salpeter equation in the Minkowski space can be reduced to a 1-dimensional equation with fixed spin-parity $J^P$ as [68],

$$i\mathcal{M}^{J^P}_{\lambda'\lambda}(\mathrm{p}', \mathrm{p}) = i\mathcal{V}^{J^P}_{\lambda',\lambda}(\mathrm{p}', \mathrm{p}) + \sum_{\lambda''}\int \frac{\mathrm{p}''^2 d\mathrm{p}''}{(2\pi)^3} \cdot i\mathcal{V}^{J^P}_{\lambda'\lambda''}(\mathrm{p}', \mathrm{p}'')G_0(\mathrm{p}'')i\mathcal{M}^{J^P}_{\lambda''\lambda}(\mathrm{p}'', \mathrm{p}), \quad (10)$$

where the sum extends only over nonnegative helicity $\lambda''$. The $G_0(\mathrm{p}'')$ is reduced from the 4-dimensional propagator under quasipotential approximation as $G_0(\mathrm{p}'') = \delta^+(p''^2_h - m^2_h)/(p''^2_l - m^2_l)$ with $p''_{h,l}$ and $m_{h,l}$ being the momenta and masses of heavy or light constituent particles. The partial wave potential is defined with the potential of interaction obtained in the above in Eq. (8) as

$$\mathcal{V}^{J^P}_{\lambda'\lambda}(\mathrm{p}', \mathrm{p}) = 2\pi\int d\cos\theta[d^J_{\lambda\lambda'}(\theta)\mathcal{V}_{\lambda'\lambda}(\boldsymbol{p}', \boldsymbol{p}) + \eta d^J_{-\lambda\lambda'}(\theta)\mathcal{V}_{\lambda'-\lambda}(\boldsymbol{p}', \boldsymbol{p})], \quad (11)$$

where $\eta = PP_1P_2(-1)^{J-J_1-J_2}$ with $P$ and $J$ being parity and spin for system, $D^{(*)}$ meson or $\Xi_c^{(*,\prime)}$ baryon. The initial and final relative momenta are chosen as $\boldsymbol{p} = (0, 0, \mathrm{p})$ and $\boldsymbol{p}' = (\mathrm{p}'\sin\theta, 0, \mathrm{p}'\cos\theta)$. The $d^J_{\lambda\lambda'}(\theta)$ is the Wigner d-matrix. We also adopt an exponential regularization by introducing a form factor into the propagator as [68] $G_0(\mathrm{p}'') \to G_0(\mathrm{p}'')[e^{-(p''^2_l - m^2_l)^2/\Lambda_r^4}]^2$ with $\Lambda_r$ being a cutoff.

## III. RESULTS AND DISCUSSIONS

With the preparation above, we can perform numerical calculation to study the molecular states from the $\Xi_c'\bar{D}^{(*)}$ and $\Xi_c^{(*)}\bar{D}^{(*)}$ interactions. After transformation of the qBSE into a matrix equation, the scattering amplitude can be obtained, and the molecular states can be searched for as the poles in the complex energy plane. As said in the Introduction, the parameters of the Lagrangians in the current work are chosen as same as those in our previous study of the hidden-charm pentaquarks [28,29]. The only parameters are cutoff $\Lambda_e$ and $\Lambda_r$, which are rewritten as a form of $\Lambda_e = \Lambda_r = m + \alpha 0.22$ GeV. Hence, in the current work, only one parameter is involved, and its value will be discussed later. In the followings, the single-channel results will be presented first. Then, the coupled-channel effects are included to produce the width of the molecular states. The couplings of molecular states to the considered channels are also discussed to analyze the contributions of decay channels.

### A. Single-channel results

For the six channels considered, the results of single-channel calculation are shown in Fig. 1. All states which can be produced in S wave with isospin $I = 0$ and 1 are considered in our calculation, that is, 20 possible molecular states will be considered.

As shown in the figure, five isoscalar bound states with spin parity $1/2^-$ are produced from the $\Xi_c^*\bar{D}^*$, $\Xi_c'\bar{D}^*$, $\Xi_c\bar{D}^*$, $\Xi_c'\bar{D}$, and $\Xi_c\bar{D}$ interactions, and four isoscalar bound states with spin parity $3/2^-$ from $\Xi_c^*\bar{D}^*$, $\Xi_c'\bar{D}^*$, $\Xi_c^*\bar{D}$, and $\Xi_c\bar{D}$ interactions. In other words, except the $\Xi_c^*\bar{D}^*$ interaction with $5/2$, bound states are produced from all other S-wave isoscalar interactions. The states appears at $\alpha$ value of about 1, and the bound energies become deeper with increasing of the $\alpha$. All bound states produced from the six channels considered are isoscalar. The isovector bound states with $I = 1$ are also searched but found difficult to be produced, even with an $\alpha$ value of about 9. It can be understood through the flavor factors in Table II. The signs of the flavor factors for isovector states reverse compared with these for isoscalar states. It is also found in the studies about the hidden-charm and hidden-bottom pentaquarks [40].

The LHCb experiment suggested that the $P_{cs}(4459)$ have a mass of about 19 MeV lower than the threshold of $\Xi_c\bar{D}^*$, which is also illustrated in Fig. 1 with the experimental uncertainty. To reproduce the experimental mass, the value of $\alpha$ about 3 should be chosen. Unfortunately, the two $\Xi_c\bar{D}^*$ states with $J^P = 1/2^-$ and $3/2^-$ have very close binding energies with single-channel calculation. Hence, we can not determine the spin parities the $P_{cs}(4459)$ in the single-channel calculation. The explicit analysis suggests that the contribution of vector exchanges are not sensitive to the spin, and the pseudoscalar exchanges are absent in

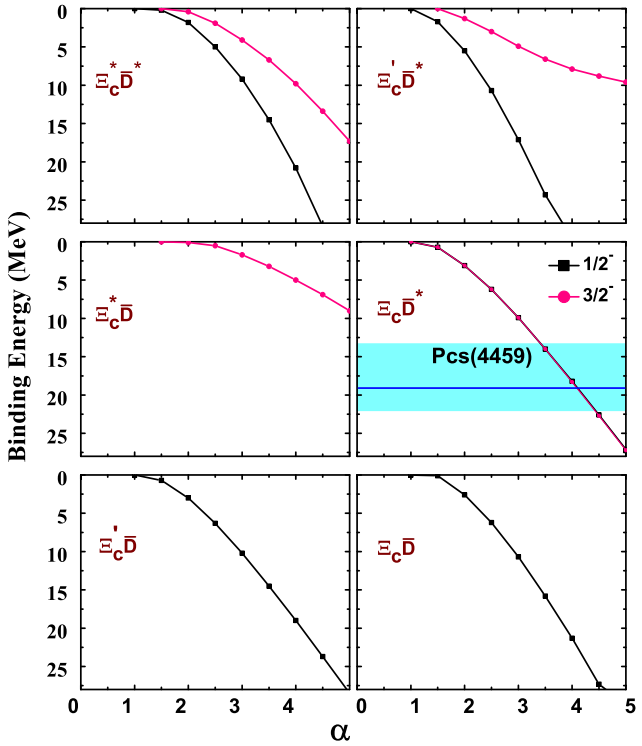


FIG. 1. The binding energies of the bound states from six single-channel interactions with the variation of parameter $\alpha$. All states carry scalar isospin $I = 0$. The thresholds of the six channels are 4654.6, 4587.4, 4513.2, 4478.0, 4446.0, 4336.6 MeV for $\Xi_c^*\bar{D}^*$, $\Xi_c'\bar{D}^*$, $\Xi_c^*\bar{D}$, $\Xi_c\bar{D}^*$, $\Xi_c'\bar{D}$, and $\Xi_c\bar{D}$, respectively. The blue line and the band are the experimental mass and uncertainties of the $P_{cs}(4459)$.

this channel as shown in Table II. The small mass gap was also suggested with single-channel calculation in Ref. [71]. It can be expected that after the pseudoscalar exchanges involved in coupled-channel effect, these two states will split.

### B. Coupled-channel results and position of poles

The single-channel calculation can provide a basic picture of the bound states from six interactions considered. Due to lack of couplings between different channels, all states are bound states, that is, the poles are at the real axis. In the followings, we will include the coupled-channel effect into the single-channel calculation. The coupled-channel results for the molecular states are listed in Table III. Here we label a pole by nearest threshold and its spin.

As listed in Table III, the poles leave the real axis after the coupled-channel effects are included, and acquire imaginary parts, which related to the width as $\Gamma = 2\mathrm{Im}z$. As in the single-channel calculation, with the increase of the parameter $\alpha$, the binding energies of all states increase. We will use the experimental mass of $P_{cs}(4459)$ to narrow the range of the $\alpha$. As in the single-channel calculation, two

TABLE III. The molecular states with coupled-channel calculation. Positions are given by the corresponding threshold subtracted by the position of a pole, $M_{th} - z$, in the unit of MeV. The $\alpha$ and the pole are in the units of GeV, and MeV, respectively. The "…" refers Not available.

| $\alpha$ | $\Xi_c^*\bar{D}^*(1/2^-)$ | $\Xi_c^*\bar{D}^*(3/2^-)$ | $\Xi_c'\bar{D}^*(1/2^-)$ | $\Xi_c'\bar{D}^*(3/2^-)$ |
|---|---|---|---|---|
| 2.0 | $1.5+0.4i$ | $0.2+0.4i$ | $5.2+1.9i$ | $1.3+2.1i$ |
| 2.5 | $3.7+1.4i$ | $2.0+4.4i$ | $6.9+4.6i$ | $1.9+5.0i$ |
| 3.0 | $7.4+3.3i$ | $N$ | $8.2+6.8i$ | $2.6+6.9i$ |
| 3.5 | $11.4+6.6i$ | $N$ | $4.9+8.7i$ | $5.6+7.3i$ |
| $\alpha$ | … | $\Xi_c^*\bar{D}(3/2^-)$ | $\Xi_c\bar{D}^*(1/2^-)$ | $\Xi_c\bar{D}^*(3/2^-)$ |
| 2.0 | … | $0.1+2.1i$ | $2.2+0.9i$ | $4.6+0.7i$ |
| 2.5 | … | $2.8+4.3i$ | $4.5+2.2i$ | $10.5+1.1i$ |
| 3.0 | … | $6.3+7.0i$ | $\mathbf{7.9+4.0i}$ | $\mathbf{19.7+1.6i}$ |
| 3.5 | … | $18.4+9.3i$ | $13.3+6.4i$ | $33.3+0.7i$ |
| $\alpha$ | $\Xi_c'\bar{D}(1/2^-)$ | … | $\Xi_c\bar{D}(1/2^-)$ | … |
| 2.0 | $4.9+0.0i$ | … | 0.2 | … |
| 2.5 | $10.8+0.0i$ | … | 3.9 | … |
| 3.0 | $19.4+0.0i$ | … | 8.5 | … |
| 3.5 | $30.9+0.0i$ | … | 14.0 | … |

poles near $\Xi_c\bar{D}^*$ threshold can be produced with spin parties $1/2^-$ and $3/2^-$, respectively. With an $\alpha$ value of about 3, the masses of these two states are close to the experimental observed values of $P_{cs}(4459)$. The widths of these two states, 8.0 and 3.2 MeV, are smaller than the experimental values. In the current work, we do not consider the experimental observation channel $\Lambda J/\psi$, which may be the origin of such small widths. A two-pole structure of the $P_{cs}(4459)$ is also helpful to explain the small widths. To give a visual picture of the results, the explicit results with $\alpha = 3$ are presented in Fig. 2, where the positions of the poles are illustrated clearly in the complex energy plane.

As shown in Fig. 2, among all states, the state $\Xi_c\bar{D}^*(3/2^-)$ is the most obvious and has the largest coverage in the complex energy plane. It should be easier to be observed in the experiment. At the $\alpha$ of 3.0, the mass of state $\Xi_c\bar{D}^*(3/2^-)$ is 4458.3 MeV, quite closing to the experimental value of the $P_{cs}(4459)$. It indicts that the $\Xi_c\bar{D}^*(3/2^-)$ state is the most possible candidate of the $P_{cs}(4459)$. And such result also confirms that a value of $\alpha$ about 3 is better to produce the experimental results. In the followings, we will take theoretical values at $\alpha$ of about 3 as the suggested values of our model. As expected, the inclusion of the coupled-channel effect makes the two states from the $\Xi_c\bar{D}^*$ interaction deviate from each other. The state with spin parity $3/2^-$ moves further while the state with $(1/2^-)$ closer to the $\Xi_c\bar{D}^*$ threshold. The higher state $\Xi_c\bar{D}^*(1/2^-)$ has a mass of 4470.1 MeV. Though two states are separated by the coupled-channel effect, the small mass gap about 10 MeV requires high precision measurement to distinguish these two states in experiment.

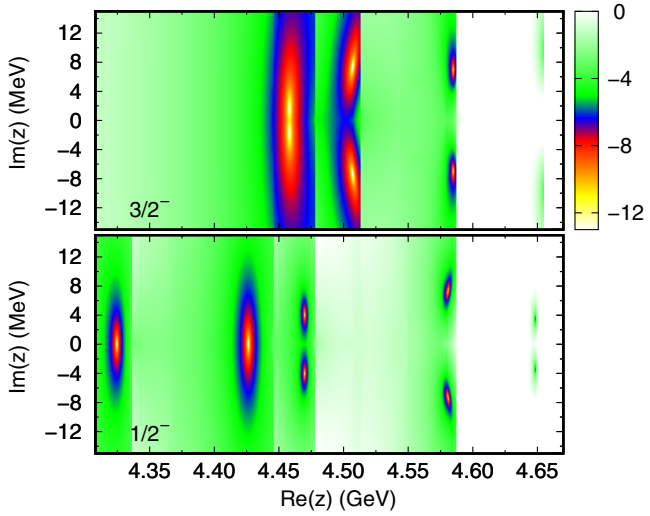


FIG. 2. The $\log|1 - V(z)G(z)|$ with the variation of $z$ for the $\Xi_c'\bar{D}^{(*)}$ and $\Xi_c^{(*)}\bar{D}^{(*)}$ interaction with $J^P = 1/2^-$ and $3/2^-$ at $\alpha = 3.0$. The color means the value of $\log|1 - V(z)G(z)|$ as shown in the color box.

With the $P_{cs}(4459)$ reproduced in our theoretical frame, we can provide the prediction of other possible strange hidden-charm molecular states. Two states with spin parity $1/2^-$ are produced near the $\Xi_c\bar{D}$ and $\Xi_c'\bar{D}$ thresholds, respectively. The lowest state has zero width because no channel lower than the $\Xi_c\bar{D}$ threshold is considered in the current work. The state near the $\Xi_c'\bar{D}$ threshold has a negligible width due to its very weak coupling to the $\Xi_c\bar{D}$ channel. No $3/2^-$ state is given here because we only consider the state which can be produced in S wave. A state can be found near the $\Xi_c^*\bar{D}$ threshold with spin parity $3/2^-$ with a width of about 14 MeV at $\alpha$ of a value 3 as shown in Table III. Two poles can also be found near the $\Xi_c'\bar{D}^*$ threshold with spin parities $1/2^-$ and $3/2^-$. The widths of these two states are similar, and the mass gap is about 5 MeV. Near the highest threshold $\Xi_c^*\bar{D}^*$, two states can be also produced from the interaction. However, as two $\Sigma_c^*\bar{D}^*$ states predicted in the hidden-charm sector [29], the signal of these two states are very weak as shown in Fig. 2. As shown in Table III, with a larger cutoff, the pole of state

TABLE IV. The positions of poles of the molecular states with two-channel calculation. Positions are given by the corresponding threshold subtracted by the position of a pole, $M_{th} - z$, in the unit of MeV. The $\alpha$ is in the unit of GeV. The "…" refers Not available.

| $\alpha$ | $\Xi_c'\bar{D}^*$ | $\Xi_c^*\bar{D}$ | $\Xi_c\bar{D}^*$ | $\Xi_c'\bar{D}$ | $\Xi_c\bar{D}$ |
|---|---|---|---|---|---|
| | | | $\Xi_c^*\bar{D}^*(1/2^-)M_{th} = 4654.6$ MeV | | |
| 2.0 | $1.7 + 0.1i$ | $1.8 + 0.1i$ | $1.8 + 0.0i$ | $1.7 + 0.2i$ | $1.8 + 0.0i$ |
| 2.5 | $4.8 + 0.2i$ | $4.9 + 0.2i$ | $4.6 + 0.1i$ | $4.2 + 0.5i$ | $4.5 + 0.0i$ |
| 3.0 | $9.0 + 0.4i$ | $9.2 + 0.5i$ | $8.3 + 0.2i$ | $7.4 + 1.4i$ | $7.6 + 0.1i$ |
| 3.5 | $14.0 + 0.6i$ | $14.5 + 0.8i$ | $12.9 + 0.3i$ | $11.3 + 2.8i$ | $11.3 + 0.2i$ |
| | | | $\Xi_c^*\bar{D}^*(3/2^-)M_{th} = 4654.6$ MeV | | |
| 2.0 | $0.2 + 0.1i$ | $0.4 + 0.0i$ | $0.1 + 0.2i$ | $0.4 + 0.0i$ | $0.4 + 0.0i$ |
| 2.5 | $1.2 + 0.7i$ | $1.5 + 0.3i$ | $0.1 + 0.3i$ | $2.0 + 0.1i$ | $1.9 + 0.0i$ |
| 3.0 | $2.7 + 1.4i$ | $2.7 + 0.8i$ | $0.1 + 2.5i$ | $4.2 + 0.1i$ | $4.1 + 0.0i$ |
| 3.5 | $4.3 + 2.3i$ | $3.7 + 1.7i$ | $0.1 + 3.1i$ | $6.9 + 0.1i$ | $6.7 + 0.0i$ |
| | | | $\Xi_c'\bar{D}^*(1/2^-)M_{th} = 4587.4$ MeV | | |
| 2.0 | … | $5.8 + 0.1i$ | $4.7 + 1.5i$ | $5.7 + 0.1i$ | $5.7 + 0.0i$ |
| 2.5 | … | $10.9 + 0.4i$ | $8.1 + 3.8i$ | $10.4 + 0.2i$ | $10.1 + 0.2i$ |
| 3.0 | … | $17.3 + 0.9i$ | $12.1 + 6.9i$ | $15.6 + 0.6i$ | $14.9 + 0.7i$ |
| 3.5 | … | $24.7 + 2.0i$ | $16.3 + 12.2i$ | $20.8 + 1.3i$ | $19.8 + 1.6i$ |
| | | | $\Xi_c'\bar{D}^*(3/2^-)M_{th} = 4587.4$ MeV | | |
| 2.0 | … | $1.6 + 0.0i$ | $0.7 + 2.1i$ | $1.8 + 0.0i$ | $1.3 + 0.3i$ |
| 2.5 | … | $3.2 + 0.1i$ | $1.3 + 5.9i$ | $3.6 + 0.0i$ | $1.8 + 1.4i$ |
| 3.0 | … | $4.9 + 0.4i$ | … | $5.4 + 0.1i$ | … |
| 3.5 | … | $6.2 + 0.6i$ | … | $7.1 + 0.1i$ | … |
| | | | $\Xi_c^*\bar{D}(3/2^-)M_{th} = 4513.2$ MeV | | |
| 2.0 | … | … | $0.1 + 1.9i$ | $0.1 + 0.0i$ | $0.1 + 0.0i$ |
| 2.5 | … | … | $0.7 + 3.7i$ | $0.5 + 0.0i$ | $0.5 + 0.0i$ |
| 3.0 | … | … | $3.9 + 5.2i$ | $1.7 + 0.0i$ | $1.7 + 0.0i$ |

*(Table continued)*

TABLE IV. *(Continued)*

| $\alpha$ | $\Xi_c'\bar{D}^*$ | $\Xi_c^*\bar{D}$ | $\Xi_c\bar{D}^*$ | $\Xi_c'\bar{D}$ | $\Xi_c\bar{D}$ |
|---|---|---|---|---|---|
| 3.5 | … | … | $11.2+6.1i$ | $3.3+0.0i$ | $3.2+0.0i$ |
| | | | $\Xi_c\bar{D}^*(1/2^-)M_{th}=4478.0$ MeV | | |
| 2.0 | … | … | … | $2.1+0.7i$ | $3.1+0.0i$ |
| 2.5 | … | … | … | $4.1+1.6i$ | $6.2+0.0i$ |
| 3.0 | … | … | … | $6.3+2.7i$ | $9.9+0.0i$ |
| 3.5 | … | … | … | $8.6+3.8i$ | $14.0+0.0i$ |
| | | | $\Xi_c\bar{D}^*(3/2^-)M_{th}=4478.0$ MeV | | |
| 2.0 | … | … | … | $3.9+0.6i$ | $3.1+0.0i$ |
| 2.5 | … | … | … | $8.2+0.9i$ | $6.2+0.0i$ |
| 3.0 | … | … | … | $13.7+1.1i$ | $9.9+0.0i$ |
| 3.5 | … | … | … | $20.5+1.2i$ | $14.0+0.0i$ |
| | | | $\Xi_c'\bar{D}(1/2^-)M_{th}=4446.0$ MeV | | |
| 2.0 | … | … | … | … | $3.0+0.0i$ |
| 2.5 | … | … | … | … | $6.3+0.0i$ |
| 3.0 | … | … | … | … | $10.2+0.0i$ |
| 3.5 | … | … | … | … | $14.5+0.0i$ |

with $3/2^-$ is even difficult to be read out from the results. These two states may be difficult to be observed in experiment.

### C. The widths of the molecular states from each decay channel

In the above, we present the widths of the states with all channels considered. The width of a molecular state is from decaying into the channels with thresholds lower than the mass of the state. The width from one of decay channels of a molecular state shows the strength of the couplings between the molecular state and the corresponding channel. By comparing the single and coupled channel results, one can find the coupled-channel effects are not very large. Hence, the main production channel of a molecular can be easily determined by the nearest threshold. In Table IV, we present the pole obtained by a two-channel calculation with main production channel and a decay channel to show the coupling of a molecular state to the decay channel. As discussed above, the theoretical values at $\alpha$ of about 3 are suggested. The results around $\alpha=3$, that is, 2.0, 2.5, 3.5, are also listed in Table IV for reference.

In the table, the results for the $\Xi_c^*\bar{D}^*$ state near the highest threshold with $1/2^-$ are listed first. Among five decay channels listed in the second to sixth columns, the strongest coupling is found in $\Xi_c'\bar{D}$ channel. The $\Xi_c\bar{D}^*$ is the most important decay channel of the $\Xi_c^*\bar{D}^*$ state with $3/2^-$, and the $\Xi_c'\bar{D}^*$ and $\Xi_c^*\bar{D}$ channels also have considerable contribution to its width. The $\Xi_c\bar{D}^*$ channel is also the main decay channel of the molecular states $\Xi_c'\bar{D}^*(3/2^-,3/2^-)$ and $\Xi_c^*\bar{D}(3/2^-)$. For the $\Xi_c\bar{D}^*$ states with $1/2^-$ and $3/2^-$, the $\Xi_c'\bar{D}$ channel is dominant to produce their widths. The $\Xi_c'\bar{D}(1/2^-)$ state couples to its only open channel $\Xi_c\bar{D}$ very weakly. Hence, the $\Xi_c\bar{D}^*$ and $\Xi_c'\bar{D}$ channels are important for the decays of four and three molecular states, respectively.

## IV. SUMMARY

In this work, the strange hidden-charm pentaquarks are studied in the molecular picture in the qBSE approach. The newly observed state $P_{cs}(4459)$ could be interpreted as the $\Xi_c\bar{D}^*(\frac{3}{2}^-)$ molecular state, which has strong coupling to the $\Xi_c'\bar{D}$ channel. The pole of this state is much more obvious in the complex energy plane than other states, which may be the reason that it was observed first. Our result does not exclude the possibility that the $P_{cs}(4459)$ is a two-peak structure composed of the $\Xi_c\bar{D}^*$ states with $1/2^-$ and $3/2^-$, which is helpful to understand the experimental width.

The current work is performed in the same theoretical frame as previous study of the hidden-charm pentaquarks with almost the same parameters [28]. Hence, the four hidden-charm pentaquarks, $P_c(4312)$, $P_c(4380)$, $P_c(4440)$, $P_c(4457)$, and the strange hidden-charm pentaquark $P_{cs}(4459)$ can be interpreted well in the molecular picture and assigned as S-wave state from the interaction of the (strange) charmed baryon and anti-charmed meson. In Ref. [71], the binding energies of $P_{cs}(4459)$ and $P_c(4312)$ were also discussed, and authors suggested that it is probably more compatible with a $\sigma$ meson that couples to all the light quarks with equal strength than with a $\sigma$ meson that does not couple with the strange quark after considering the mixing of the singlet and octet scalar mesons. In the current work, we adopt a coupling constant without coupling with the strange quark. However, the cutoff is introduced to reflect the internal structure of

hadron, which is determined by the experimental results. It makes the discussion as in Ref. [71] impracticable in the current work. It is interesting to consider it in future work if we have more experimental information.

In the same model, we also predict other possible strange hidden-charm pentaquarks. Two states with spin parity $1/2^-$ are predicted near the $\Xi_c'\bar{D}$ and $\Xi_c\bar{D}$ thresholds, respectively. Since the decay channels of these two states are less than other states, their widths may be smaller. Near the $\Xi_c^*\bar{D}$ threshold, an obvious pole can be found in the complex energy plane with $3/2^-$. This state couples strongly with $\Xi_c\bar{D}$ channel. As two states near the $\Xi_c\bar{D}^*$ threshold, one can find two states with $1/2^-$ and $3/2^-$ near the $\Xi_c'\bar{D}^*$ threshold, which have strong coupling to the $\Xi_c\bar{D}^*$ channel. The poles can also be found near the highest threshold $\Xi_c^*\bar{D}^*$. Such poles are dimly in the complex energy plane, and may be difficult to be find in experiment. The experimental research of those states are helpful to understand the origin of the $P_{cs}$ and $P_c$ states.

## ACKNOWLEDGMENTS

This project is supported by the National Natural Science Foundation of China (Grants No. 11675228).

[1] R. Aaij *et al.* (LHCb Collaboration), Evidence of a $J/\psi\Lambda$ structure and observation of excited $\Xi^-$ states in the $\Xi_b^- \to J/\psi\Lambda K^-$ decay, arXiv:2012.10380.
[2] R. Aaij *et al.* (LHCb Collaboration), Observation of $J/\psi p$ Resonances Consistent with Pentaquark States in $\Lambda_b^0 \to J/\psi K^- p$ Decays, Phys. Rev. Lett. **115**, 072001 (2015).
[3] J. J. Wu, R. Molina, E. Oset, and B. S. Zou, Prediction of Narrow $N^*$ and $\Lambda^*$ Resonances with Hidden Charm above 4 GeV, Phys. Rev. Lett. **105**, 232001 (2010).
[4] Z. C. Yang, Z. F. Sun, J. He, X. Liu, and S. L. Zhu, The possible hidden-charm molecular baryons composed of anti-charmed meson and charmed baryon, Chin. Phys. C **36**, 6 (2012).
[5] W. L. Wang, F. Huang, Z. Y. Zhang, and B. S. Zou, $\Sigma_c\bar{D}$ and $\Lambda_c\bar{D}$ states in a chiral quark model, Phys. Rev. C **84**, 015203 (2011).
[6] C. W. Xiao, J. Nieves, and E. Oset, Combining heavy quark spin and local hidden gauge symmetries in the dynamical generation of hidden charm baryons, Phys. Rev. D **88**, 056012 (2013).
[7] R. Chen, X. Liu, X. Q. Li, and S. L. Zhu, Identifying Exotic Hidden-Charm Pentaquarks, Phys. Rev. Lett. **115**, 132002 (2015).
[8] H. X. Chen, W. Chen, X. Liu, T. G. Steele, and S. L. Zhu, Towards Exotic Hidden-Charm Pentaquarks in QCD, Phys. Rev. Lett. **115**, 172001 (2015).
[9] M. Karliner and J. L. Rosner, New Exotic Meson and Baryon Resonances from Doubly-Heavy Hadronic Molecules, Phys. Rev. Lett. **115**, 122001 (2015).
[10] L. Roca, J. Nieves, and E. Oset, LHCb pentaquark as a $\bar{D}^*\Sigma_c - \bar{D}^*\Sigma_c^*$ molecular state, Phys. Rev. D **92**, 094003 (2015).
[11] J. He, $\bar{D}\Sigma_c^*$ and $\bar{D}^*\Sigma_c$ interactions and the LHCb hidden-charmed pentaquarks, Phys. Lett. B **753**, 547 (2016).
[12] T. J. Burns, Phenomenology of $P_c(4380)^+$, $P_c(4450)^+$ and related states, Eur. Phys. J. A **51**, 152 (2015).
[13] S. G. Yuan, K. W. Wei, J. He, H. S. Xu, and B. S. Zou, Study of $qqqc\bar{c}$ five quark system with three kinds of quark-quark hyperfine interaction, Eur. Phys. J. A **48**, 61 (2012).
[14] R. F. Lebed, The pentaquark candidates in the dynamical diquark picture, Phys. Lett. B **749**, 454 (2015).
[15] L. Maiani, A. D. Polosa, and V. Riquer, The new pentaquarks in the diquark model, Phys. Lett. B **749**, 289 (2015).
[16] X. H. Liu, Q. Wang, and Q. Zhao, Understanding the newly observed heavy pentaquark candidates, Phys. Lett. B **757**, 231 (2016).
[17] R. Aaij *et al.* (LHCb Collaboration), Observation of a Narrow Pentaquark State, $P_c(4312)^+$, and of Two-Peak Atructure of the $P_c(4450)^+$, Phys. Rev. Lett. **122**, 222001 (2019).
[18] M. Z. Liu, Y. W. Pan, F. Z. Peng, M. Sánchez Sánchez, L. S. Geng, A. Hosaka, and M. P. Valderrama, Emergence of a Complete Heavy-Quark Spin Symmetry Multiplet: Seven Molecular Pentaquarks in Light of the Latest LHCb Analysis, Phys. Rev. Lett. **122**, 242001 (2019).
[19] M. L. Du, V. Baru, F. K. Guo, C. Hanhart, U. G. Meißner, J. A. Oller, and Q. Wang, Interpretation of the LHCb $P_c$ States as Hadronic Molecules and Hints of a Narrow $P_c(4380)$, Phys. Rev. Lett. **124**, 072001 (2020).
[20] M. L. Du, V. Baru, F. K. Guo, C. Hanhart, U. G. Meißner, J. A. Oller, and Q. Wang, Revisiting the nature of the $P_c$ pentaquarks, arXiv:2102.07159.
[21] R. Chen, Z. F. Sun, X. Liu, and S. L. Zhu, Strong LHCb evidence supporting the existence of the hidden-charm molecular pentaquarks, Phys. Rev. D **100**, 011502 (2019).
[22] H. X. Chen, W. Chen, and S. L. Zhu, Possible interpretations of the $P_c(4312)$, $P_c(4440)$, and $P_c(4457)$, Phys. Rev. D **100**, 051501 (2019).
[23] C. Fernández-Ramírez *et al.* (JPAC Collaboration), Interpretation of the LHCb $P_c(4312)^+$ Signal, Phys. Rev. Lett. **123**, 092001 (2019).
[24] Q. Wu and D. Y. Chen, Production of $P_c$ states from $\Lambda_b$ decay, Phys. Rev. D **100**, 114002 (2019).
[25] Y. Huang, J. He, H. F. Zhang, and X. R. Chen, Discovery potential of hidden charm baryon resonances via photoproduction, J. Phys. G **41**, 115004 (2014).
[26] Z. G. Wang, Analysis of the $P_c(4312)$, $P_c(4440)$, $P_c(4457)$ and related hidden-charm pentaquark states with QCD sum rules, Int. J. Mod. Phys. **35**, 2050003 (2020).

[27] H. Huang, J. He, and J. Ping, Looking for the hidden-charm pentaquark resonances in $J/\psi p$ scattering, arXiv:1904.00221.

[28] J. He, Study of $P_c(4457)$, $P_c(4440)$, and $P_c(4312)$ in a quasipotential Bethe-Salpeter equation approach, Eur. Phys. J. C **79**, 393 (2019).

[29] J. He and D. Y. Chen, Molecular states from $\Sigma_c^{(*)}\bar{D}^{(*)} - \Lambda_c\bar{D}^{(*)}$ interaction, Eur. Phys. J. C **79**, 887 (2019).

[30] Y. H. Lin and B. S. Zou, Strong decays of the latest LHCb pentaquark candidates in hadronic molecule pictures, Phys. Rev. D **100**, 056005 (2019).

[31] C. J. Xiao, Y. Huang, Y. B. Dong, L. S. Geng, and D. Y. Chen, Exploring the molecular scenario of Pc(4312), Pc(4440), and Pc(4457), Phys. Rev. D **100**, 014022 (2019).

[32] J. He, Internal structures of the nucleon resonances N(1875) and N(2120), Phys. Rev. C **91**, 018201 (2015).

[33] J. He, Nucleon resonances $N(1875)$ and $N(2100)$ as strange partners of LHCb pentaquarks, Phys. Rev. D **95**, 074031 (2017).

[34] Y. H. Lin, C. W. Shen, and B. S. Zou, Decay behavior of the strange and beauty partners of $P_c$ hadronic molecules, Nucl. Phys. **A980**, 21 (2018).

[35] J. Wu, Y. R. Liu, K. Chen, X. Liu, and S. L. Zhu, Hidden-charm pentaquarks and their hidden-bottom and $B_c$-like partner states, Phys. Rev. D **95**, 034002 (2017).

[36] X. Y. Wang, J. He, and X. Chen, Systematic study of the production of hidden-bottom pentaquarks via $\gamma p$ and $\pi^- p$ scatterings, Phys. Rev. D **101**, 034032 (2020).

[37] H. Huang and J. Ping, Investigating the hidden-charm and hidden-bottom pentaquark resonances in scattering process, Phys. Rev. D **99**, 014010 (2019).

[38] G. Yang, J. Ping, and J. Segovia, Hidden-bottom pentaquarks, Phys. Rev. D **99**, 014035 (2019).

[39] B. Wang, L. Meng, and S. L. Zhu, Hidden-charm and hidden-bottom molecular pentaquarks in chiral effective field theory, J. High Energy Phys. 11 (2019) 108.

[40] J. T. Zhu, S. Y. Kong, Y. Liu, and J. He, Hidden-bottom molecular states from $\Sigma_b^{(*)}B^{(*)} - \Lambda_b B^{(*)}$ interaction, Eur. Phys. J. C **80**, 1016 (2020).

[41] V. V. Anisovich, M. A. Matveev, J. Nyiri, A. V. Sarantsev, and A. N. Semenova, Nonstrange and strange pentaquarks with hidden charm, Int. J. Mod. Phys. A **30**, 1550190 (2015).

[42] Z. G. Wang, Analysis of the $\frac{1}{2}^{\pm}$ pentaquark states in the diquark–diquark–antiquark model with QCD sum rules, Eur. Phys. J. C **76**, 142 (2016).

[43] A. Feijoo, V. K. Magas, A. Ramos, and E. Oset, A hidden-charm $S = -1$ pentaquark from the decay of $\Lambda_b$ into $J/\psi, \eta\Lambda$ states, Eur. Phys. J. C **76**, 446 (2016).

[44] J. X. Lu, E. Wang, J. J. Xie, L. S. Geng, and E. Oset, The $\Lambda_b \to J/\psi K^0\Lambda$ reaction and a hidden-charm pentaquark state with strangeness, Phys. Rev. D **93**, 094009 (2016).

[45] H. X. Chen, L. S. Geng, W. H. Liang, E. Oset, E. Wang, and J. J. Xie, Looking for a hidden-charm pentaquark state with strangeness S=-1 from $\Xi_b^-$ decay into $J/\psi K^-\Lambda$, Phys. Rev. C **93**, 065203 (2016).

[46] R. Chen, J. He, and X. Liu, Possible strange hidden-charm pentaquarks from $\Sigma_c^{(*)}\bar{D}_s^*$ and $\Xi_c^{(\prime,*)}\bar{D}^*$ interactions, Chin. Phys. C **41**, 103105 (2017).

[47] C. W. Xiao, J. Nieves, and E. Oset, Prediction of hidden charm strange molecular baryon states with heavy quark spin symmetry, Phys. Lett. B **799**, 135051 (2019).

[48] Q. Zhang, B. R. He, and J. L. Ping, Pentaquarks with the $qqs\bar{Q}Q$ configuration in the chiral quark model, arXiv:2006.01042.

[49] B. Wang, L. Meng, and S. L. Zhu, Spectrum of the strange hidden charm molecular pentaquarks in chiral effective field theory, Phys. Rev. D **101**, 034018 (2020).

[50] K. Azizi, Y. Sarac, and H. Sundu, Investigation of $P_{cs}(4459)^0$ pentaquark via its strong decay to $\Lambda J/\Psi$, arXiv:2101.07850.

[51] H. X. Chen, W. Chen, X. Liu, and X. H. Liu, Establishing the first hidden-charm pentaquark with strangeness, arXiv:2011.01079.

[52] F. Z. Peng, M. J. Yan, M. Sánchez Sánchez, and M. P. Valderrama, The $P_{cs}(4459)$ pentaquark from a combined effective field theory and phenomenological perspectives, arXiv:2011.01915.

[53] Z. G. Wang, Analysis of the $P_{cs}(4459)$ as the hidden-charm pentaquark state with QCD sum rules, arXiv:2011.05102.

[54] R. Chen, Can the newly $P_{cs}(4459)$ be a strange hidden-charm $\Xi_c\bar{D}^*$ molecular pentaquarks? Phys. Rev. D **103**, 054007 (2021).

[55] J. A. Oller and U. G. Meissner, Chiral dynamics in the presence of bound states: Kaon nucleon interactions revisited, Phys. Lett. B **500**, 263 (2001).

[56] D. Jido, J. A. Oller, E. Oset, A. Ramos, and U. G. Meissner, Chiral dynamics of the two Lambda(1405) states, Nucl. Phys. **A725**, 181 (2003).

[57] L. Roca, E. Oset, and J. Singh, Low lying axial-vector mesons as dynamically generated resonances, Phys. Rev. D **72**, 014002 (2005).

[58] L. S. Geng, E. Oset, L. Roca, and J. A. Oller, Clues for the existence of two K(1)(1270) resonances, Phys. Rev. D **75**, 014017 (2007).

[59] M. Albaladejo, P. Fernandez-Soler, F. K. Guo, and J. Nieves, Two-pole structure of the $D_0^*(2400)$, Phys. Lett. B **767**, 465 (2017).

[60] H. Y. Cheng, C. Y. Cheung, G. L. Lin, Y. C. Lin, T. M. Yan, and H. L. Yu, Chiral Lagrangians for radiative decays of heavy hadrons, Phys. Rev. D **47**, 1030 (1993).

[61] T. M. Yan, H. Y. Cheng, C. Y. Cheung, G. L. Lin, Y. C. Lin, and H. L. Yu, Heavy quark symmetry and chiral dynamics, Phys. Rev. D **46**, 1148 (1992); Erratum, **55**, 5851 (1997).

[62] M. B. Wise, Chiral perturbation theory for hadrons containing a heavy quark, Phys. Rev. D **45**, R2188 (1992).

[63] R. Casalbuoni, A. Deandrea, N. Di Bartolomeo, R. Gatto, F. Feruglio, and G. Nardulli, Phenomenology of heavy meson chiral Lagrangians, Phys. Rep. **281**, 145 (1997).

[64] Y. R. Liu and M. Oka, $\Lambda_c N$ bound states revisited, Phys. Rev. D **85**, 014015 (2012).

[65] M. Tanabashi *et al.* (Particle Data Group), Review of particle physics, Phys. Rev. D **98**, 030001 (2018).

[66] C. Isola, M. Ladisa, G. Nardulli, and P. Santorelli, Charming penguins in $B \to K^*\pi, K(\rho, \omega, \phi)$ decays, Phys. Rev. D **68**, 114001 (2003).

[67] A. F. Falk and M. E. Luke, Strong decays of excited heavy mesons in chiral perturbation theory, Phys. Lett. B **292**, 119 (1992).

[68] J. He, The $Z_c(3900)$ as a resonance from the $D\bar{D}^*$ interaction, Phys. Rev. D **92**, 034004 (2015).

[69] J. He, Study of the $B\bar{B}^*/D\bar{D}^*$ bound states in a Bethe-Salpeter approach, Phys. Rev. D **90**, 076008 (2014).

[70] J. He, D. Y. Chen, and X. Liu, New Structure Around 3250 MeV in the Baryonic B Decay and the $D_0^*(2400)N$ Molecular Hadron, Eur. Phys. J. C **72**, 2121 (2012).

[71] M. J. Yan, F. Z. Peng, M. Sánchez Sánchez, and M. P. Valderrama, Axial meson exchange and the $Z_c(3900)$ and $Z_{cs}(3985)$ resonances as heavy hadron molecules, arXiv: 2102.13058.